
Learning Smooth Representation for Unsupervised Domain Adaptation

Guanyu Cai, Yuqin Wang, Lianghua He

Department of Computer Science and Technology
Tongji University
Shanghai, China 201804

{caiguanyu, 1710836, helianghua@tongji.edu.cn}

Abstract

In unsupervised domain adaptation, existing methods utilizing the boundary decision have achieved remarkable performance, but they lack analysis of the relationship between decision boundary and features. In our work, we propose a new principle that adaptive classifiers and transferable features can be obtained in the target domain by learning smooth representations. We analyze the relationship between decision boundary and ambiguous target features in terms of smoothness. Thereafter, local smooth discrepancy is defined to measure the smoothness of a sample and detect sensitive samples which are easily misclassified. To strengthen the smoothness, sensitive samples are corrected in feature space by optimizing local smooth discrepancy. Moreover, the generalization error upper bound is derived theoretically. Finally, We evaluate our method in several standard benchmark datasets. Empirical evidence shows that the proposed method is comparable or superior to the state-of-the-art methods and local smooth discrepancy is a valid metric to evaluate the performance of a domain adaptation method.

1 Introduction

The performance of various computer vision problems has been significantly improved with the development of deep convolutional neural networks (CNN) [11]. However, a precondition of this improvement is that numerous labeled samples are needed and test samples are drawn from the same distribution with training ones. Once there exists a *dataset shift* between the training and test samples, the performance of a CNN model decreases dramatically [4, 1]. In order to tackle this problem, unsupervised domain adaptation (UDA) transfers knowledge from a labeled source domain to an unlabeled target domain.

A bunch of classical UDA methods is to match moments of features in the source and target domains. They regard moments of a distribution as the main characteristics [28, 26, 15]. By matching moments, they hope to match distributions of different domains. Other kinds of remarkable UDA methods are based on adversarial training strategy. [5] first introduces a domain classifier to make distributions of distinct domains matching. [14, 2] also propose methods which are effective based on such a principle. However, these methods ignore the effect of a decision boundary. Alignment of distributions does not ensure that target samples are well-classified. The relationship between the decision boundary and target samples is also important.

[24, 16, 17] regard the output of softmax function as complementary information to train a UDA model. These methods still focus on matching distributions of different domains, but the influence of decision boundary is considered. Moreover, MCD [24] explains that misclassification in the target domain is caused by ambiguous target features near the decision boundary and proposes a siamese-like network to overcome this phenomenon. These methods achieve excellent performance

and their philosophies are illustrated clearly. However, the reason why a decision boundary robust in the source domain becomes invalid in the target domain is not well explained.

In this work, we give a new point of view to explain why a decision boundary is ill in the target domain. In our opinion, the smoothness of target samples is the key to model performance. Therefore, we define a non-negative function named **local smooth discrepancy** to measure the smoothness of a sample. Finally, a optimization schedule based on local smooth discrepancy is proposed to tackle the UDA problem.

In particular, we observe the phenomenon that performance drop in the target domain is similar to the overfitting problem. It is common for deep learning models because of extreme nonlinearity. In UDA problem, a dataset shift between different domains intensifies the overfitting. A popular belief based on widely observed facts is that the law of designing a model with good generalization ability is described by smoothness [18]. Based on this principle, we explain how a dataset shift and smoothness affect the performance in the target domain. Further, we define a formula named local smooth discrepancy to measure the smoothness of a target sample. Two specific computing method are introduced. Utilizing local smooth discrepancy, we propose a detailed training strategy to tackle the UDA problem. The model contains a feature generator and classifier. The classifier tries to classify source samples correctly and detect sensitive target samples which are easily misclassified. The principle used to detect sensitive samples is that they are not smooth with respect to the classifier. The feature generator is trained to strengthen the smoothness of these sensitive samples. In other words, we seek samples that are not smooth and modify them to be smooth. Note that we add no auxiliary network which is common in MCD [24] and adversarial training methods [5, 16].

2 Related Work

A theoretical work proposed in [1] confirms that a discrepancy between the source and target distributions causes a model invalid in the target domain. Because the distribution of a domain is difficult to illustrate, intuitive thought is to match moments of distributions instead. [15] matches expectations of features. [26] takes covariance of features into consideration. Moreover, [28] utilizes high-order moments to align distributions of different domains. These methods perform well in numerous settings.

As DANN [5] proposed, methods based on adversarial training become popular gradually. These methods introduce a domain classifier to predict which domain a sample is drawn from. At the same time, a feature generator is trained to fool the domain classifier so that features from different domains are matched. [27] follows this philosophy and implements adversarial training in feature space. Several methods implement adversarial training in pixel level [20, 2, 14]. These methods try to generate target images from labeled source images. In this way, a classification model is able to be trained with labeled target images. Specifically, PixelDA [2] follows the training strategy of generative adversarial networks (GANs) and obtains excellent performance on digits datasets. [20, 14] introduce training strategy similar to cycle GAN to improve their performance.

However, an essential factor, the decision boundary, is ignored in these methods. They only take the marginal distributions into consideration while neglect the information contained in prediction. In order to solve this problem, JAN [17] modifies DAN [15] to match joint distributions. CADA [16] subtly changes the training strategy of DANN [5] and achieves remarkable results. ATDA [23] adds two auxiliary classifiers to assist in generating valid pseudo labels for target samples. It constructs decision boundaries for target domain in two different views. Moreover, MCD [24] gives us a concise explanation of why matching marginal distributions still causes misclassification. It also proposes a siamese-like network and adversarial training strategy to solve the UDA problem. MCD [24] is comparable or superior to the existing methods on several benchmark domain adaptation datasets.

3 Preliminary

In this section, we give a brief description of UDA and define several notions. In the context of vanilla UDA, source images and corresponding labels $\{X_s, Y_s\}$ are drawn from the underlying joint source distribution $P_s(X_s, Y_s)$. Meanwhile, there is a set of unlabeled target images $\{X_t\}$ drawn from a marginal target distribution $P_t(X_s)$. The goal of a UDA task is to train a model with $\{X_s, Y_s\}$ and $\{X_t\}$ to predict target labels $\{Y_t\}$ of $\{X_t\}$. In practical settings, we only access to finite samples

where a source domain $\{x_s^i, y_s^i\}_i^{N_s}$ consists of N_s samples and target domain $\{x_t^j\}_j^{N_t}$ consists of N_t samples.

In our setting, the trained model f is composed of a feature generator G and classifier C . G takes inputs x_s or x_t and the generated features z_s or z_t are feeded into C to classify them into different classes. Because of a dataset shift between the source and target domain, f which achieves a low source risk $R_S = \mathbb{E}_{x_s, y_s \sim P_s} [C(G(x_s)) \neq y_s]$ can easily result in an unsatisfied target risk $R_T = \mathbb{E}_{x_t, y_t \sim P_t} [C(G(x_t)) \neq y_t]$. Thus, the goal of UDA methods is narrow down to reduce R_t .

4 Learning Smooth Representation

4.1 Main Idea

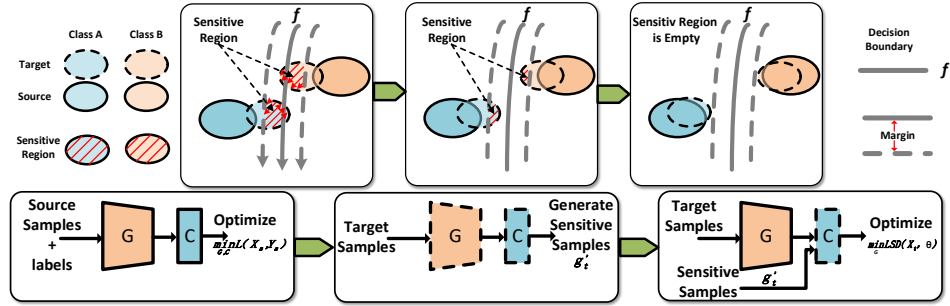


Figure 1: A visual illustration of how the proposed method achieves adaptation. **(Upper)** The left block explains why dataset shift between different domains causes misclassification. The other two blocks depict the process of forming a robust margin between target samples and the decision boundary. At the same time, distributions of the target and source domains are matched. **(Lower)** The optimization schedule is able to project sensitive samples to new locations away from the decision boundary in three steps. Dashed lines indicate fixed network parameters.

Previous UDA methods, such as moments alignment ones [26, 15] or adversarial training ones [5, 27], aim to completely match the feature distributions between different domains. Although they all have achieved excellent performance on various tasks, the decision boundary which implies the determinacy of predictions is ignored. MCD [24] has taken it into consideration and discussed it in their specific network architecture which is similar to a siamese network. In this work, we consider a more general setting that a classification network f is only composed of a feature generator G and classifier C . As shown in Figure 1, a f well-trained in the source domain is able to classify source samples correctly. For a robust model, there is a large margin between the decision boundary and samples. However, a dataset shift across different domains results in a probability that a set of target samples would cross the boundary decided by source domain. These samples are misclassified. Therefore, we regard samples near the decision boundary as sensitive ones which easily lead errors to f . It is similar to the overfitting problem which is common in deep learning models. The extreme nonlinearity of deep neural networks leads to a phenomenon that performance drop happens when facing out-of-distribution samples. In UDA problem, the dataset shift further exacerbates this situation. A large number of target samples are regarded as out-of-distribution samples for f . In order to obtain a f work well in the target domain, G needs to project x_t into feature space far away from the decision boundary.

An intuitive solution to form a large margin between target samples and the source decision boundary is to detect samples close to the boundary and force G project them far away from the boundary. As shown in Figure 1, we could observe a phenomenon that samples near the decision boundary are less smooth than those far away from the boundary. In detail, the smoothness in our setting means that a sample and the samples around it should belong to the same category. Therefore, if a sample is in close proximity to the decision boundary, samples in the neighborhood are inevitable to cross the boundary so that the smoothness is broken down. On the contrary, samples away from the boundary are robust to keep the smoothness. This observation indeed inspires us to design a specific algorithm for UDA problem. We tend to define a concrete formula to measure the smoothness of a sample. Sensitive samples are able to be detected with it, and then G is trained to project them far

away from the boundary. In other words, they become smooth. We give a visual illustration of this procedure in Figure 1. As you can see, not only the dataset shift between source and target domain is reduced, but also source and target samples achieve a large margin with the decision boundary. The ideal smooth representations of both domains are learned in our method. An interesting point is that promoting smoothness of a model is a typical principle to alleviate the overfitting problem. However, a regularization term is the common way for overfitting problem while we design a novel optimization schedule to tackle the UDA problem.

4.2 Local Smooth Discrepancy

According to the definition of smoothness in our setting, we define a concrete formula named **local smooth discrepancy** (LSD) to measure it:

$$LSD(x, \theta) = D(C(G(x) + r), C(G(x))), \text{ where } \|r\| \leq \epsilon \quad (1)$$

where θ denotes all the parameters of a model. r denotes a noise added to the output of G , and ϵ denotes the maximum norm of r . $D(\cdot, \cdot)$ is a discrepancy function that measures the divergence between two outputs of C . In $LSD(x, \theta)$, a feature vector $\mathbf{g} = G(x)$ adds r to detect another feature vector \mathbf{g}' in \mathbf{g} 's neighborhood. ϵ controls the range of sampling in \mathbf{g} 's neighborhood. As for the choice of $D(\cdot, \cdot)$, we employ cross-entropy loss function in all experiments.

Although LSD is well-defined, there is still an essential point we should pay more attention. Specifically, r is limited only by its norm in (1) and its direction is ignored. In fact, the goal of adding r includes detecting sensitive samples. If a \mathbf{g} is close to the decision boundary and all \mathbf{g}' belong to the same category with \mathbf{g} , it means that the direction of r could not detect sensitive samples. In this condition, sensitive samples are not modified to be away from the boundary and a robust margin between target samples and the decision boundary is unable to be formed. In order to solve this problem, we propose two plans to produce r , an isotropic one and an anisotropic one.

Isotropic Plan In the isotropic plan, we draw r from a Gaussian distribution and normalize it to satisfy $r \leq \epsilon$. Because r is isotropic, there must be a considerable number of \mathbf{g}' are closer to the decision boundary than the corresponding \mathbf{g} . Thus, for the \mathbf{g} nearby the boundary, several \mathbf{g}' broken down the smoothness are detected. The formula of LSD is modified into:

$$LSD(x, \theta) = D(C(G(x) + r_{ran}), C(G(x))), \text{ where } r_{ran} = \frac{m}{\|m\|_2}, m \sim N(0, 1) \quad (2)$$

Anisotropic Plan Anisotropic plan only looks for r which drag \mathbf{g} closer to the decision boundary and ignores r in other directions. To reach this goal, we take the insight from adversarial attack [7]. Adversarial attack applies a certain hardly perceptible perturbation, which is found by maximizing the model's prediction error, to an image to cause the model misclassify [7]. This philosophy fits well with our goal which tries to seek some noise to make the consequential feature vectors belong to different classes. However, these perturbations are found in image level and true labels are needed. In UDA problem, true labels for the target domain is unreachable. Moreover, in our setting, perturbations are added in feature space. Therefore, we make several modifications in traditional adversarial attack methods. In detail, traditional adversarial attack methods approximate adversarial perturbation by:

$$r_{adv} \approx \epsilon \frac{m}{\|m\|_2}, \text{ where } m = \nabla_x D(C(G(x)), y) \quad (3)$$

Instead, we approximate it by:

$$r_{adv} \approx \epsilon \frac{m}{\|m\|_2}, \text{ where } m = \nabla_{\mathbf{g}} D(C(\mathbf{g}), \text{onehot}(C(\mathbf{g}))), \mathbf{g} = G(x) \quad (4)$$

where *onehot* denotes transforming the softmax output of C to a one-hot vector. (4) computes gradients of \mathbf{g} in the feature space instead of image space and replaces y with *onehot*($C(\mathbf{g})$). These modifications result in a new LSD for anisotropic noise:

$$LSD(x, \theta) = D(C(G(x) + r_{adv}), C(G(x))) \quad (5)$$

4.3 Optimization for Local Smooth Discrepancy

After defining the local smooth discrepancy, we design a optimization schedule to follow our motivation. We seek sensitive samples that violate the smoothness rule, and train G to project them into smooth locations.

First, we train G and C in the source domain to obtain the decision boundary which is crucial to the following steps.

$$\min_{G,C} \mathcal{L}(X_s, Y_s), \text{ where } \mathcal{L}(X_s, Y_s) = \mathbb{E}_{x_s, y_s \sim P_s} \left[\sum_{k=1}^K \mathbb{1}[k = y_s] \log C(G(x_s)) \right] \quad (6)$$

where $\mathbb{1}[\cdot]$ is an indicator function, and K denotes that there are K classes in a task. Then, we produce sensitive samples based on the decision boundary. Note that supervised learning in (6) is able to form robust margin between source samples and the decision boundary so that we focus on target samples in this step. In our work, sensitive samples \mathbf{g}'_t are generated in the feature space of G :

$$\mathbf{g}'_t = \mathbf{g}_t + r \quad (7)$$

where $\mathbf{g}_t = G(x_t)$, and r is a general notation for the adding noise. In practice, we set $r = r_{ran}$ for an isotropic plan or $r = r_{adv}$ for an anisotropic plan. Finally, we train G to minimize local smooth discrepancy for target samples. Only parameters of G are updated in this step. G is trained to project \mathbf{g}'_t to the same category with \mathbf{g}_t :

$$\min_G LSD(X_t, \theta_G), \text{ where } LSD(X_t, \theta_G) = \mathbb{E}_{x_t \sim P_t} D(C(\mathbf{g}'_t), C(\mathbf{g}_t)) \quad (8)$$

where θ_G denotes parameters of G , and $D(\cdot, \cdot)$ denotes cross-entropy loss function. (6) (7) and (8) are repeated in the optimization schedule as shown in Figure 1.

4.4 Generalization Error Bound

In this section, we analyze theoretically the reason why the proposed method works well in the target domain. Ben-David proposed the theory that bounds the expected error in the target domain $R_T(h)$ [1]. There are three terms compose $R_T(h)$, expected error in the source domain $R_S(h)$, $\mathcal{H}\Delta\mathcal{H}$ distance that measures the discrepancy between source and target domains, and a combined error of the ideal joint hypothesis λ .

Theorem 1 [1] *Let \mathcal{H} be the hypothesis class. Suppose that \mathcal{H} is symmetric(i.e., $h \in \mathcal{H}$ implies $-h \in \mathcal{H}$). Given two domains S and T , for any $h \in \mathcal{H}$, we have:*

$$R_T(h) \leq R_S(h) + \frac{1}{2} d_{\mathcal{H}\Delta\mathcal{H}}(S, T) + \lambda$$

$$\text{where } d_{\mathcal{H}\Delta\mathcal{H}}(S, T) = 2 \sup_{h, h' \in \mathcal{H}} |\mathbb{E}_{x \sim S} \mathbb{1}[h(x) \neq h'(x)] - \mathbb{E}_{x \sim T} \mathbb{1}[h(x) \neq h'(x)]|, \quad (9)$$

$$\lambda = \min(R_S(h) + R_T(h))$$

where $R_T(h)$ and $R_S(h)$ are the errors of hypothesis h in the corresponding domain. $\mathbb{1}[\cdot]$ denotes a indicator function.

According to [1], $R_S(h)$ is extremely small with supervised learning and λ is also negligible if a UDA problem is solvable. Thus, we concentrate on minimizing $d_{\mathcal{H}\Delta\mathcal{H}}(S, T)$. Regarding $d_{\mathcal{H}\Delta\mathcal{H}}(S, T)$, because of reachable true labels of the source domain, h and h' are able to classify source samples correctly and $\mathbb{E}_{x \sim S} \mathbb{1}[h(x) \neq h'(x)]$ is assumed to be low. Thus, to approximate $d_{\mathcal{H}\Delta\mathcal{H}}(S, T)$, we need to approximate $\sup_{h, h' \in \mathcal{H}} \mathbb{E}_{x \sim T} \mathbb{1}[h(x) \neq h'(x)]$.

Actually, MCD [24] train two different classifier to be inconsistent in the target domain to reach the supremum of $\mathbb{E}_{x \sim T} \mathbb{1}[h(x) \neq h'(x)]$. However, in our method, we try to approximate it without an auxiliary classifier h' . Assume that there exists an ideal $h^* = \arg \min_h \lambda$ so that $R_T(h^*)$ is extremely

low. If there is a set of sensitive samples $x' \in T'$ which is also drawn from $P_t(X_t)$ and can easily lead wrong results from h , $d_{\mathcal{H}\Delta\mathcal{H}}(S, T)$ is well-approximated by $\mathbb{E}_{x' \in T'} \mathbb{1}[h^*(x') \neq h(x')]$. According to [18], both the proposed isotropic and anisotropic plans are able to produce x' that follow $P_t(X_t)$ and leads inconsistent results from h . Therefore, we regard generated sensitive samples as T' in our method. In practice, since $h^*(x')$, $x' \in T'$ is unavailable, we replace it with $h(x)$, $x \in T$. Note that x' is generated from corresponding x and their labels are the same, so this replacement is reasonable. Finally, this term is approximated by:

$$d_{\mathcal{H}\Delta\mathcal{H}}(S, T) \approx \mathbb{E}_{x \in T, x' \in T'} \mathbb{1}[h(x) \neq h(x')] \quad (10)$$

In fact, (10) is a discrete way to measure the smoothness of target samples. In order to optimize a model with SGD, we propose local smooth discrepancy $LSD(x, \theta) = D(C(G(x) + r), C(G(x)))$ to replace $\mathbb{E}_{x \in T, x' \in T'} \mathbb{1}[h(x) \neq h(x')]$ as the objective function. In addition, although the manner that we use pseudo labels of $h(x)$ to replace unreachable $h^*(x')$ is unlikely to guarantee the real $d_{\mathcal{H}\Delta\mathcal{H}}(S, T)$ to be obtained, the iterative optimization and increasing accuracy of h during training ensure our method works well.

5 Experiments

In order to verify the effectiveness of the proposed method (SRDA), we conduct several classification experiments on standard benchmark datasets. First, we test SRDA on several digits classification datasets which are the most common datasets for UDA. Then, we test it on a more complex and massive dataset, VisDA [22], to show the advanced performance of SRDA. Finally, we analyze the effectiveness of local smooth discrepancy in two settings. In all experiments, we implement models with Pytorch, and employ the optimization schedule we propose.

5.1 Digits Classification

We evaluate four types of adaptation scenarios by utilizing the digits datasets, MNIST [12], USPS [10], Synthetic Traffic Signs (SYNSIG) [19], Street View House Numbers (SVHN) [21] and German Traffic Signs Recognition Benchmark (GTSRB) [25]. Specifically, MNIST, USPS and SVHN consist of 10 classes, whereas SYNSIG and GTSRB are traffic sign datasets which consist of 43 classes. In this experiment, we set four transfer tasks: SVHN→MNIST, SYNSIG→GTSRB, MNIST→USPS and USPS→MNIST. In detail, the dataset shift in SVHN→MNIST is caused by a different property of an image that SVHN contains RGB images while MNIST contains grayscale images. The shift between USPS and MNIST is relatively small because both of them are handwritten digit datasets and contain grayscale images. Images in SYNSIG and GTSRB have distinct properties because those in SYNSIG are synthesized and the rest is collected from the real world. For a fair comparison, we follow the protocols provided in MCD [24] and ADDA [27].

Table 1: Classification accuracy percentage of digits classification experiment among all four tasks. The first row corresponds to the performance if no adaption is implemented. We evaluate three SRDA models with different plans for adding noise. The results are cited from each study.

Method	SVHN	SYNSIG	MNIST	USPS
	→ MNIST	→ GTSRB	→ USPS	→ MNIST
Source Only	67.1	85.1	76.7	63.4
DAN	71.1	91.1	-	-
DANN	71.1	88.7	77.1	73.0
DSN	82.7	93.1	91.3	-
ADDA	76.0	-	89.4	90.1
CoGAN	-	-	91.2	89.1
ATDA	86.2	96.2	-	-
ASSC	95.7	82.8	-	-
DRCN	82.0	-	91.8	73.7
MCD	96.2	94.4	94.2	94.1
SRDA(FGSM)	93.73	90.46	80.29	95.25
SRDA(VAT)	95.10	89.45	76.85	95.49
SRDA(RAN)	98.81	89.28	93.42	94.46

In this experiment, in order to verify the robustness of SRDA, we implement both isotropic and anisotropic plans. For the isotropic plan, we sample noise from a standard Gaussian distribution. In all four tasks, hyper-parameter ϵ is set to 0.5 and the learning rate is $1e^{-3}$. For the anisotropic plan, sensitive samples are generated in two different ways. We choose two classical adversarial attack algorithm, namely FGSM [7] and VAT [18], to produce noise adding to a feature vector. Note that FGSM [7] needs true labels to execute a backpropagation to compute gradients, so that we use pseudo labels to replace them. Except for MNIST→USPS, ϵ is set to 0.5 in the other three tasks. In

MNIST→USPS, ϵ is set to 0.3. We set batch size to 128 in all tasks for both plans and all models are trained for 150 epochs. Learning rate is set to $1e^{-4}$ for FGSM plan while $1e^{-3}$ for VAT plan.

Results of the digits classification experiment are shown in Table 1. We compare our three SRDA models, namely SRDA (FGSM), SRDA (VAT) and SRDA (RAN), with other state-of-the-art UDA algorithms such as DAN [15], DANN [5], DSN [3], ADDA [27], CoGAN [14], ATDA [23], ASSC [8], DRCN [6] and MCD [24]. Among all four tasks, SRDA ranks first in two of them. Especially in USPS→MNIST which is the most difficult task, our three models are the top three. Only MCD is comparable to them and other methods are inferior to ours with a large margin. In SVHN→MNIST, SRDA (RAN) ranks first and other two models are the top five. In the other two tasks, our models do not obtain the best results. We conclude that it is caused by the relative satisfying results when no adaptation is implemented. Once a model without adaptation allocates target samples away from the decision boundary, SRDA is hard to detect enough sensitive samples to optimize G . Thus, SRDA is unable to improve the baseline a lot in this setting. The fact that improvement in SYNSIG→GTSRB which is the easiest setting is the smallest verifies our conclusion.

5.2 VisDA Classification

Table 2: Classification accuracy percentage of VisDA classification experiment. The first row corresponds to the performance if no adaption is implemented. Columns in the middle correspond to different categories and the column on the right represents average accuracy. We evaluate three SRDA models with different plans for adding noise. The number behind MCD denotes different hyper-parameters. The results are cited from each study.

Method	Pl	Bc	Bs	Ca	Hr	Kf	Mc	Ps	Pt	Sk	Tr	Tk	Avg
No UDA	55.1	53.3	61.9	59.1	80.6	17.9	79.7	31.2	81.0	26.5	73.5	8.5	52.4
DAN	87.1	63.0	76.5	42.0	90.3	42.9	85.9	53.1	49.7	36.3	85.8	20.7	61.1
DANN	81.9	77.7	82.8	44.3	81.2	29.5	65.1	28.6	51.9	54.6	82.8	7.8	57.4
MCD(2)	81.1	55.3	83.6	65.7	87.6	72.7	83.1	73.9	85.3	47.7	73.2	27.1	69.7
MCD(3)	90.3	49.3	82.1	62.9	91.8	69.4	83.8	72.8	79.8	53.3	81.5	29.7	70.6
MCD(4)	87.0	60.9	83.7	64.0	88.9	79.6	84.7	76.9	88.6	40.3	83.0	25.8	71.9
SRDA(F)	90.1	67.0	82.3	56.0	84.8	88.2	90.3	77.0	82.5	26.8	85.0	16.2	71.1
SRDA(V)	89.4	43.5	81.2	60.2	81.1	57.6	93.7	76.6	81.8	41.3	79.6	22.0	69.5
SRDA(R)	90.9	74.8	81.9	59.1	87.5	77.3	89.9	79.4	85.3	40.6	85.1	21.6	73.3

We further assess SRDA on a more complex object classification dataset. VisDA [22] in this experiment constructs an adaptation from synthetic-object to real-object images. It contains more than 280K images belonging to 12 categories. These images are divided into training, validation and test sets. There are 152,397 training images synthesized by rendering 3D models with different angles and lighting conditions. The validation images are collected from MSCOCO [13] and amount to 55,388 in total. In this experiment, we regard the training set as a source domain and the validation set as a target domain. Similarly, in order to ensure fairness, we utilize the same backbone network, ResNet101 [9], with MCD [24]. The setting of generator and classifier networks is also the same. In addition, we also employ the entropy minimization trick which is used in MCD [24].

In this experiment, we also implement both isotropic and anisotropic plans. For the anisotropic plan, FGSM [7] and VAT [18] algorithms are implemented. All models are trained for 15 epochs and batch size is set to 32. Learning rate is set to $1e^{-4}$. Similarly, we compare SRDA (FGSM), SRDA (VAT) and SRDA (RAN) with several typical methods, such as DAN [15], DANN [5], and MCD [24] which is the state-of-the-art method.

Results of the VisDA classification experiment are shown in Table 2. SRDA and MCD [24] achieve much better accuracy than other methods. Moreover, SRDA (RAN) ranks first among all the models and SRDA (FGSM) obtains comparable accuracy with MCD [24]. In detail, SRDA (RAN) achieves the best results in class plane and person, SRDA (VAT) achieves the best result in class motor cycle and SRDA (FGSM) gets the best result in class knife. An interesting phenomenon is that three models of SRDA perform diversely among these categories. For example, in class knife, SRDA (FGSM) performs much better than the others and SRDA (VAT) ranks first in class motor cycle. Overall, SRDA (RAN) performs best. This reflects the importance of detecting sensitive samples. A well-defined plan which could seek more sensitive samples and a metric which could illustrate the smoothness of samples precisely are hopeful to further promote the proposed method.

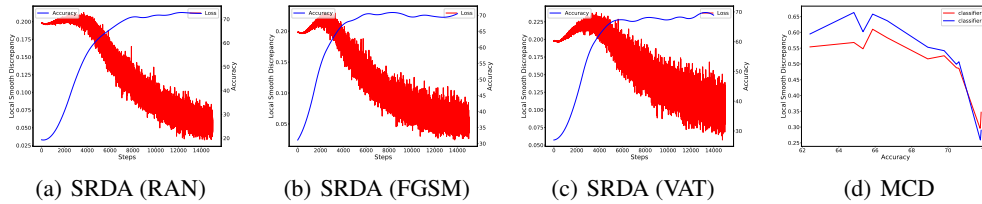


Figure 2: Three figures on the left display relationship between LSD (red line) and accuracy (blue line) during the training period. Three SRDA models are evaluated on VisDA. As discrepancy decreases, the accuracy increases. The figure on the right display relationship between LSD and accuracy in MCD. The model with higher accuracy gets a lower LSD.

5.3 Discuss of Local Smooth Discrepancy

In order to verify that LSD we defined indeed reflects the smoothness of a sample and the performance of a model, we show the relationship between LSD and accuracy in Figure 2. Three models, SRDA (RAN), SRDA (FGSM) and SRDA (VAT), are assessed on VisDA. We follow the settings in VisDA classification experiment. Note that because we get the accuracy every epoch and LSD is recorded every step, we show the accuracy after a quadratic interpolation.

As shown in Figure 2(a), 2(b), and 2(c), the accuracy of all three models gradually increases as LSD decreases. This indicates that the proposed local smooth discrepancy is a reasonable metric to evaluate the performance of a UDA model. As is shown in Table 2, SRDA (RAN) performs best on VisDA, SRDA (FGSM) ranks second and SRDA (VAT) is the worst model among them. In fact, the order of performance on VisDA also corresponds to LSD. SRDA (VAT) shows the highest loss, SRDA (RAN) obtains the lowest loss and SRDA (FGSM) ranks in the middle. The result verifies that smoothness is a key factor that affects the performance of a UDA model. Our explanation of performance drop in the target domain based on smoothness is also confirmed.

Moreover, to prove that LSD is a general metric to assess the performance of a UDA model, we further test it on MCD with different accuracy. In this experiment, we follow the settings described in MCD [24] and train models on VisDA. Overall, we train 12 MCD models with different accuracy by tuning hyper-parameters. As LSD is not the objective function of MCD, we introduce the original FGSM algorithm to generate adversarial samples on image level. Traditional white adversarial attack algorithms generate samples with their own networks. This paradigm introduces a new variable that adversarial samples are not the same for different MCD models. Thus, we generate adversarial samples with SRDA (RAN) in this experiment to ensure fairness for each MCD model. ϵ is also set to 0.5. With these adversarial images, LSD is calculated with their corresponding images in the target domain. To ensure the validity of the results, both classifiers in MCD are tested.

As is shown in Figure 2(d), there is an obvious relationship between LSD and accuracy that a low LSD corresponds to high accuracy. We train 12 MCD models with accuracy belongs to $\{62.42, 64.83, 65.33, 65.86, 66.66, 68.89, 69.79, 70.46, 70.60, 71.76, 71.78, 71.82\}$. LSD of both classifiers gradually decreases from 0.6 to 0.3 roughly. This means that LSD is a reasonable general metric to evaluate the performance of a UDA model. However, there are also several MCD model with high accuracy showing relative high LSD. We argue that the randomness of the gradient descent algorithm causes this fluctuation.

6 Conclusion

In this paper, we propose a novel method for UDA problem. We introduce the definition of smoothness in UDA problem and explain the reason for performance drop in the target domain in terms of smoothness. According to the definition, we propose a formula named local smooth discrepancy to measure the smoothness of samples which can both detect sensitive samples and be an optimized objective function. Based on these, we give a concise training strategy to train a UDA model and a theoretical analysis is given. We extensively evaluate our method on several benchmark datasets. In almost all experiments, our method is comparable or superior to the state-of-the-art methods.

References

- [1] Shai Ben-David, John Blitzer, Koby Crammer, Alex Kulesza, Fernando Pereira, and Jennifer Wortman Vaughan. A theory of learning from different domains. *Machine learning*, 79(1-2):151–175, 2010.
- [2] Konstantinos Bousmalis, Nathan Silberman, David Dohan, Dumitru Erhan, and Dilip Krishnan. Unsupervised pixel-level domain adaptation with generative adversarial networks. In *Proceedings of the IEEE Conference on Computer Vision and Pattern Recognition*, pages 3722–3731, 2017.
- [3] Konstantinos Bousmalis, George Trigeorgis, Nathan Silberman, Dilip Krishnan, and Dumitru Erhan. Domain separation networks. In D. D. Lee, M. Sugiyama, U. V. Luxburg, I. Guyon, and R. Garnett, editors, *Advances in Neural Information Processing Systems 29*, pages 343–351. Curran Associates, Inc., 2016.
- [4] Jeff Donahue, Yangqing Jia, Oriol Vinyals, Judy Hoffman, Ning Zhang, Eric Tzeng, and Trevor Darrell. Decaf: A deep convolutional activation feature for generic visual recognition. In *International Conference on Machine Learning*, pages 647–655, 2014.
- [5] Yaroslav Ganin, Evgeniya Ustinova, Hana Ajakan, Pascal Germain, Hugo Larochelle, François Laviolette, Mario Marchand, and Victor Lempitsky. Domain-adversarial training of neural networks. *The Journal of Machine Learning Research*, 17(1):2096–2030, 2016.
- [6] Muhammad Ghifary, W. Bastiaan Kleijn, Mengjie Zhang, David Balduzzi, and Wen Li. Deep reconstruction-classification networks for unsupervised domain adaptation. In *ECCV (4)*, volume 9908 of *Lecture Notes in Computer Science*, pages 597–613. Springer, 2016.
- [7] Ian J Goodfellow, Jonathon Shlens, and Christian Szegedy. Explaining and harnessing adversarial examples. *arXiv preprint arXiv:1412.6572*, 2014.
- [8] Philip Haeusser, Thomas Frerix, Alexander Mordvintsev, and Daniel Cremers. Associative domain adaptation. In *The IEEE International Conference on Computer Vision (ICCV)*, Oct 2017.
- [9] Kaiming He, Xiangyu Zhang, Shaoqing Ren, and Jian Sun. Deep residual learning for image recognition. In *Proceedings of the IEEE Conference on Computer Vision and Pattern Recognition*, pages 770–778, 2016.
- [10] Jonathan J. Hull. A database for handwritten text recognition research. *IEEE Transactions on Pattern Analysis and Machine Intelligence*, 16(5):550–554, 1994.
- [11] Alex Krizhevsky, Ilya Sutskever, and Geoffrey E Hinton. Imagenet classification with deep convolutional neural networks. In *Advances in Neural Information Processing Systems*, pages 1097–1105, 2012.
- [12] Yann LeCun, Léon Bottou, Yoshua Bengio, Patrick Haffner, et al. Gradient-based learning applied to document recognition. *Proceedings of the IEEE*, 86(11):2278–2324, 1998.
- [13] Tsung-Yi Lin, Michael Maire, Serge Belongie, James Hays, Pietro Perona, Deva Ramanan, Piotr Dollár, and C Lawrence Zitnick. Microsoft coco: Common objects in context. In *European Conference on Computer Vision*, pages 740–755. Springer, 2014.
- [14] Ming-Yu Liu and Oncel Tuzel. Coupled generative adversarial networks. In *Advances in Neural Information Processing Systems*, pages 469–477, 2016.
- [15] Mingsheng Long, Yue Cao, Jianmin Wang, and Michael Jordan. Learning transferable features with deep adaptation networks. In Francis Bach and David Blei, editors, *Proceedings of the 32nd International Conference on Machine Learning*, volume 37 of *Proceedings of Machine Learning Research*, pages 97–105, Lille, France, 07–09 Jul 2015. PMLR.
- [16] Mingsheng Long, Zhangjie Cao, Jianmin Wang, and Michael I Jordan. Conditional adversarial domain adaptation. In *Advances in Neural Information Processing Systems*, pages 1640–1650, 2018.

- [17] Mingsheng Long, Han Zhu, Jianmin Wang, and Michael I Jordan. Deep transfer learning with joint adaptation networks. In *Proceedings of the 34th International Conference on Machine Learning-Volume 70*, pages 2208–2217. JMLR. org, 2017.
- [18] Takeru Miyato, Shin-ichi Maeda, Shin Ishii, and Masanori Koyama. Virtual adversarial training: a regularization method for supervised and semi-supervised learning. *IEEE Transactions on Pattern Analysis and Machine Intelligence*, 2018.
- [19] Boris Moiseev, Artem Konev, Alexander Chigorin, and Anton Konushin. Evaluation of traffic sign recognition methods trained on synthetically generated data. In *International Conference on Advanced Concepts for Intelligent Vision Systems*, pages 576–583. Springer, 2013.
- [20] Zak Murez, Soheil Kolouri, David Kriegman, Ravi Ramamoorthi, and Kyungnam Kim. Image to image translation for domain adaptation. In *Proceedings of the IEEE Conference on Computer Vision and Pattern Recognition*, pages 4500–4509, 2018.
- [21] Yuval Netzer, Tao Wang, Adam Coates, Alessandro Bissacco, Bo Wu, and Andrew Y Ng. Reading digits in natural images with unsupervised feature learning. 2011.
- [22] Xingchao Peng, Ben Usman, Neela Kaushik, Judy Hoffman, Dequan Wang, and Kate Saenko. Visda: The visual domain adaptation challenge. *arXiv preprint arXiv:1710.06924*, 2017.
- [23] Kuniaki Saito, Yoshitaka Ushiku, and Tatsuya Harada. Asymmetric tri-training for unsupervised domain adaptation. In Doina Precup and Yee Whye Teh, editors, *Proceedings of the 34th International Conference on Machine Learning*, volume 70 of *Proceedings of Machine Learning Research*, pages 2988–2997, International Convention Centre, Sydney, Australia, 06–11 Aug 2017. PMLR.
- [24] Kuniaki Saito, Kohei Watanabe, Yoshitaka Ushiku, and Tatsuya Harada. Maximum classifier discrepancy for unsupervised domain adaptation. In *Proceedings of the IEEE Conference on Computer Vision and Pattern Recognition*, pages 3723–3732, 2018.
- [25] Johannes Stalkamp, Marc Schlipsing, Jan Salmen, and Christian Igel. The german traffic sign recognition benchmark: A multi-class classification competition. In *IJCNN*, volume 6, page 7, 2011.
- [26] Baochen Sun and Kate Saenko. Deep coral: Correlation alignment for deep domain adaptation. In *European Conference on Computer Vision*, pages 443–450. Springer, 2016.
- [27] Eric Tzeng, Judy Hoffman, Kate Saenko, and Trevor Darrell. Adversarial discriminative domain adaptation. In *Proceedings of the IEEE Conference on Computer Vision and Pattern Recognition*, pages 7167–7176, 2017.
- [28] Werner Zellinger, Thomas Grubinger, Edwin Lughofer, Thomas Natschläger, and Susanne Saminger-Platz. Central moment discrepancy (cmd) for domain-invariant representation learning. *International Conference on Learning Representations*, 2017.